Physics Letters B 761 (2016) 469–474

Contents lists available at ScienceDirect

Physics Letters B

www.elsevier.com/locate/physletb

Elastic scattering in geometrical model

Zbigniew Plebaniak [a,*], Tadeusz Wibig [a,b]

[a] National Centre for Nuclear Research, Astrophysics Division, Cosmic Ray Laboratory, ul. 28 Pułku Strzelców Kaniowskich 69, 90-558 Łódź, Poland
[b] Faculty of Physics and Applied Informatics, University of Łódź, ul. Pomorska 149/153, 90-236 Łódź, Poland

ARTICLE INFO

Article history:
Received 20 May 2016
Received in revised form 31 August 2016
Accepted 31 August 2016
Available online 6 September 2016
Editor: L. Rolandi

Keywords:
Elastic scattering
Optical model
Cross section
Cosmic rays

ABSTRACT

The experimental data on proton–proton elastic and inelastic scattering emerging from the measurements at the Large Hadron Collider, calls for an efficient model to fit the data. We have examined the optical, geometrical picture and we have found the simplest, linear dependence of this model parameters on the logarithm of the interaction energy with the significant change of the respective slopes at one point corresponding to the energy of about 300 GeV. The logarithmic dependence observed at high energies allows one to extrapolate the proton–proton elastic, total (and inelastic) cross sections to ultra high energies seen in cosmic rays events which makes a solid justification of the extrapolation to very high energy domain of cosmic rays and could help us to interpret the data from an astrophysical and a high energy physics point of view.

1. Introduction

The process of elastic scattering of hadrons has been studied experimentally in a wide energy region for more than half a century. In the 1960's with the available center of mass (c.m.s.) energies of $\sqrt{s} = 4$–6 GeV it was found that the conventional "diffraction cone" mechanism failed what was clearly visible at larger transferred momenta. Additional data at the energies of $\sqrt{s} = 19$, 20, 23, 28, 31, 45, 53, 62 GeV were published in the middle of 70's. At the end of the previous millennium the range of available energies ends around 2 TeV. Only recently the results of the TOTEM collaboration at the LHC on elastic pp scattering processes at $\sqrt{s} = 7$ TeV were published [9,12].

The measurements at the LHC at 7 TeV c.m.s. collision energy set the next point on an energy scale where the optical model of hadrons can be examined. The observed so far evolution of the proton shadow profile and the energy dependence of the parameters describing its shape could be extended towards the limit of the ultra high-energy cosmic rays (UHECR), where important questions of physics and astrophysics are still unanswered. It is expected that the answers could be linked (also) to some extent to the value of the proton–proton cross sections at around 10^{20} eV of laboratory energy.

Many phenomenological models of proton have been proposed. As it is said by Dremlin in Ref. [39] *[....] "Most of them aspire to be 'a phenomenology of everything' related to elastic scattering of hadrons in a wide energy range. Doing so in the absence of applicable laws and methods of the fundamental theory, they have to use a large number of adjustable parameters. The free parameters have been determined by fitting the model results to the available experimental data." [...] Independent of their success and failure, we are sure that, "in the long run, the physical picture may be expected to be much more important than most of the detailed computations".* (the last citation is from the 1969 paper by Cheng and Wu published in the first volume of Phys. Rev. D [36]).

2. Phenomenology of the scattering process

The elastic scattering amplitude $F(s,t)$ describing the proton–proton scattering

$$\frac{d\,\sigma_{el}}{d|t|} = \pi\,|F(t)|^2 \quad , \tag{1}$$

could be parameterized in many ways starting from the simple exponential $\exp(Bt)$ proposed already in 1964 by Orear in Ref. [54]. New data allows for more sophisticated form. It was proposed by Barger and Phillips [56] in 1973 in the form

$$F(s,t) = i\left[\sqrt{A(s)}e^{\frac{1}{2}B(s)t} + \sqrt{C(s)}e^{\phi(s)}e^{\frac{1}{2}D(s)t}\right] \quad , \tag{2}$$

which can be used for 7 TeV LHC scattering data explicitly [45,50], or modified, as proposed, e.g., in Ref. [42]

* Corresponding author.
E-mail address: zp@zpk.u.lodz.pl (Z. Plebaniak).

http://dx.doi.org/10.1016/j.physletb.2016.08.064

Table 1
The extrapolated cross sections in mb at higher energies.

Energy ($\sqrt{s}$)	14 TeV	24 TeV	30 TeV	57 TeV	95 TeV
Fagundes et al. [41]	108.6 ± 1.2				
Bourelly et al. [27]	103.63 ± 1.0				
Petrov et al. [55]	106.73				
Block, Halzen et al. [26]	107.30				
Islam et al. [48]	110.00				
Jenkovszky et al. [50]	111.00				
Block [22]				133.40 ± 1.6	
AKENO [53]	104 ± 26	124 ± 34			
Fly's Eye [18]			120 ± 15		
AUGER [3]				133.20 ± 13	
Telescope Array [1]					170.00 ± 50
This work	**105.56**	**115.8**	**120.33**	**132.66**	**143.09**

$$F(s,t) = i\left[\sqrt{A(s)}e^{\frac{1}{2}B(s)t}G(s,t) + \sqrt{C(s)}e^{\phi(s)}e^{\frac{1}{2}D(s)t}\right] \ , \tag{3}$$

or in the number of possibilities inspected by Khoze, Martin and Ryskin in Ref. [51].

A different modification was proposed by Menon and collaborators in Ref. [35] who consider the parameterization of the scattering amplitude as a sum of Orear exponentials [54]:

$$F(s,t) = \sum_{i=1}^{n} \alpha_i e^{\beta_i t} \ . \tag{4}$$

They obtained, with the summation of up to six components, perfect fits to the ISR data from 19.4 GeV to 62.4 GeV [40]. Their 'model-independent' analysis of elastic proton–proton scattering data [16,17,40] was extended to higher energies and the parameters α_i and β_i were expressed as functions of the available c.m.s. energy. Predictions for LHC were given there and are listed in the Table 1.

On the other hand the absorption processes can be naturally studied in a geometrical framework. The correspondence between interaction geometry and the momentum transfer space is defined with the Fourier transform with the help of the profile function $\Gamma(s,b)$ (or the eikonal Ω)

$$F(s,t) = i\int_0^\infty J_0\left(b\sqrt{-t}\right)\,\Gamma(s,b)\,b\,db \ = \\ = i\int_0^\infty J_0\left(b\sqrt{-t}\right)\,\{1-\exp\left[-\Omega(s,b)\right]\}\,b\,db \ . \tag{5}$$

This gives the possibility to apply the form-factor formalism to the hadron interaction $\Omega(s,t) = C(s)G_p(t)G_p(t)$ where $C(s)$ works for the absorption coefficient.

$$\Omega(s,b) \ = \ (1-i\alpha)\int_0^\infty J_0(qb)\,G_{p,E}^2(t)\,\frac{f(t)}{f(0)}\,q\,dq \ , \tag{6}$$

($q = \sqrt{-t}$). This formalism has been proposed and developed by Bourrely, Soffer and Wu since late 70's [28–30] using

$$G_{p,E}(t) = \frac{1}{\left(1-t/m_1^2\right)\left(1-t/m_2^2\right)} \ , \\ f(t) = f(0)\,\frac{a^2+t}{a^2-t} \ . \tag{7}$$

The initial simple model with six free parameters (at high energies) becomes at the LHC energies much more complicated [31]. The asymptotic form has been eventually estimated and compared with the numerical results in Ref. [27].

The pure geometrical picture of proton scattering and the relation of the scattering amplitude to the transmission coefficient ($|\Omega|$) appears already in 1968 in the paper by Chou and Yang [37]. The main point there is to find the (mean) opaqueness, which may be, in general, a complex-valued function, for the given value of the impact parameter. It is quite natural to assume that the hadron has the internal structure defined by the density function $\rho(x,y,z)$. Taking z as a collision axis we can define a hadron profile

$$D(\mathbf{b}) = \int_{-\infty}^{\infty} \rho(x,y,z)\,dz \ , \tag{8}$$

and for two colliding hadrons the convolution is

$$\Omega(b) = \Omega(\mathbf{b}) = iK_{pp}\iint_{-\infty}^{\infty} D(\mathbf{b}-\mathbf{b}')D(\mathbf{b}')\,d^2\mathbf{b}' \ . \tag{9}$$

Any particular model could be fully characterized by the generalized opacity: the eikonal function Ω (in the impact parameter space) as it is written in Eq. (5). Its particular shape can be obtained using dipole electromagnetic form factors like it is done, for example, in Ref. [37] similar to the one given in Eq. (7).

Another interesting way of introducing Ω is to use the evolution of the imaginary part of the profile function $\Gamma(s,b) = 1 - \exp\left[-\Omega(s,b)\right]$ which could be, according to Ref. [34], determined using the nonlinear differential logistic equation. The concept is that it includes, in a natural way, saturation effects expected as energy grows. This assumption leads to

$$\Gamma(s,b) \ = \ \frac{1}{e^{(b-b_0)/\gamma}+1} \ , \tag{10}$$

where b_0 and γ are proton radial scale parameters which define the cross section scaling properties. A very similar profile function was found as a special case of the model of Rybczyński and Włodarczyk where shapes of colliding protons are defined by the event-by-event fluctuations of the radius of the proton in the 'black disk' picture [57]. If the fluctuations are negligible the black disk limit is retained, while for the cross section fluctuations described by the gamma distribution, another extreme is obtained: the Gaussian proton profile.

Introducing new scaling variable $\hat{b} = b/b_0(s)$ to Eq. (10) the proton profile satisfies the (modified) geometrical scaling (if γ/b_0 is constant)

$$\frac{d\sigma_{\rm el}}{dt} \ \sim \ b_0^2\left[\ f\left(|t|\,b_0^2\right)\right]^2 \ , \tag{11}$$

and eventually the scattering picture tends to the black disk limit when the energy goes to infinity ($b_0 \to \infty$): $\sigma_{\text{tot.}} \sim \sigma_{\text{el.}} \sim b_0^2$ ($\sigma_{\text{el.}}/\sigma_{\text{tot.}} = 1/2$).

In the paper by Islam, Luddy and Prokudin [49] the profile function $\Gamma(s,b)$ was chosen arbitrarily [47]

$$\Gamma(b,s) = g(s)\left[\frac{1}{1+e^{(b-b_0)/\gamma}} + \frac{1}{1+e^{-(b+b_0)/\gamma}} - 1\right] . \tag{12}$$

The comparison of Eq. (12) with Eq. (10) shows an interesting similarity. The results of the Islam model agree with the measured data above ISR energies quite well [49], however, at 7 TeV the agreement is not as perfect [44].

It is known for a long time, that the geometrical scaling holds below ISR energies ($\sqrt{s} < 20$ GeV). The analysis by Brogueira and Dias de Deus [34] shows that starting from the highest ISR energy the proton appears to be getting blacker and edgier already, in SPS at $\sqrt{s} = 200$ GeV it becomes quite clear and this tendency continuously becomes more visible as the energy grows.

In the series of papers of Block and co-workers there is proposed the "Aspen model" [21,25]. The eikonal function Ω in this model is a sum of four separate components related to individual qq gg, gq interactions and the oddeon exchange

$$\Omega(s,b) = i\left[\sigma_{\text{qq}}(s)A(b,\mu_{\text{qq}}) + \sigma_{\text{gg}}(s)A(b,\mu_{\text{gg}}) + \right.$$
$$\left. + \sigma_{\text{qg}}(s)A(b,\mu_{\text{qg}}) + \sigma_{\text{odd}}(s)A(b,\mu_{\text{odd}})\right] , \tag{13}$$

with $A(b,\mu) \sim K_3(\mu b)$. The model is used mainly for the estimation and extrapolation of the total (elastic and inelastic) cross sections to extremely high energies. Its agreement with high energy scattering data is not perfect, as it is shown in [24] for LHC 7 TeV. The modified Bessel function appears in the Aspen model as a result of convolutions of the hadron densities distributed again [37] in the way which leads to dipole electromagnetic form factor from similar to the one shown in Eq. (7).

3. The modification of the simplest model

The predictions for the simplest models of hadrons are well known (see, e.g., Ref. [23]). From the geometrical point of view, the general picture is such that protons become blacker, edgier and larger (BEL) [46]. One of the simplest and quite obvious hadronic matter distributions is the exponential one

$$\rho_h(\mathbf{r}) = \frac{m_h^3}{8\pi} e^{-m_h|\mathbf{r}|} . \tag{14}$$

The complex form of the eikonal could be defined using the λ factor which defines the ratio of the real to the imaginary part of the Ω

$$\lambda(s) = \frac{\Re(\Omega(b,s))}{\Im(\Omega(b,s))} . \tag{15}$$

The energy dependence of λ has been known quite accurately for a long time and it was smoothly parameterized, e.g., by Menon in Refs. [40,52]. For the present calculation we have slightly modified this solution. In Fig. 1 our dependency of $\rho(s)$ is shown in comparison with selected data.

The exponential form of Eq. (14) has been used in Ref. [58] and the results of scattering cross section were given there. In general the agreement with the data is seen below and at the region of the first dip ($|t| < 0.7$ GeV^2). The diffractive-like picture of the scattering differential cross section is rather satisfactory there, but the deficit of higher momenta transfers ($|t| > 1$ GeV^2) is the essential defect of the simple model in general. To obtain the solution closer to the high $p_\perp$ experimental distribution we have examined a slightly more sophisticated hadronic mass distribution: we

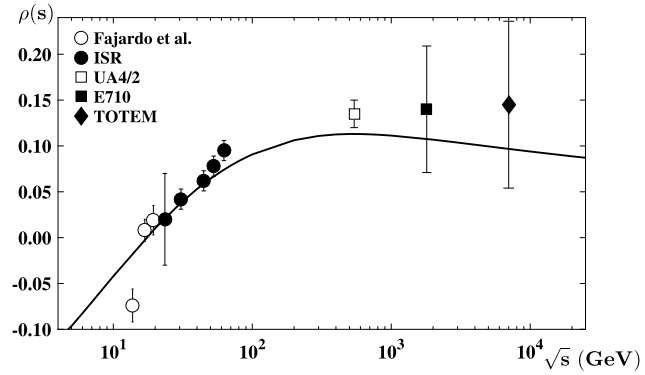

Fig. 1. Ratio of the real and the imaginary part of the scattering amplitude $\rho = \Re(F(b,s))/\Im(F(b,s))$. Solid curve is the result of the parameterization of $\lambda(s)$ from Ref. [40,52] modified slightly by us used in the present work. Points represent data from [6,8,11,14,43].

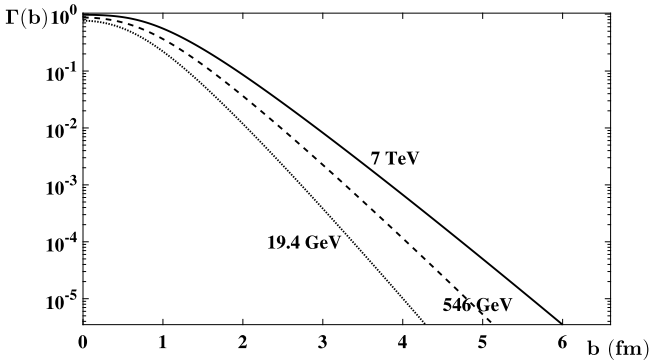

Fig. 2. Profile functions for three energies ($\sqrt{s} = 19$ GeV, 546 GeV and 7 TeV) used in the paper.

have used instead of the one exponential distribution the sum of two with distinct exponents m_1 and m_2 and different normalization factors c_1 and c_2.

$$\rho_h(\mathbf{r}) = \frac{1}{8\pi}\left(c_1 m_1^3 e^{-m_1|\mathbf{r}|} + c_2 m_2^3 e^{-m_2|\mathbf{r}|}\right) . \tag{16}$$

The four parameters of the distribution proposed in Eq. (16) are the subject of the fitting procedure. The values of m_1 and m_2 are not much different from each other, as well as the values of c_1 and c_2 and the profiles obtained eventually from Eq. (14) and these adjusted using Eq. (16) are quite similar. The profiles obtained in the present work at three specific and characteristic energies (low – 19 GeV, high, the middle SPS: 546 GeV, and recent LHC 7 TeV) are shown, as examples in Fig. 2. Presented profile functions $\Gamma(b)$ are described by following equation:

$$\Gamma(b) = 1 - e^{-\Omega(b)} , \tag{17}$$

where $\Omega(b)$ is calculated using Eq. (9).

Multicomponent geometrical models of high energy scattering appear as a result of the decomposition of the interacting nucleon into constituents of different nature, which could have, thus, different distributions on the impact parameter plane. In "Aspen model" of Block and Halzen [26], interacting protons are compounds of quarks and gluons. This approach leads to the three (qq, gg and qg) different parts of the high energy eikonal profile function, see Eq. (13).

Another idea which leads to the two component system is the one proposed by Bialas and Bzdak [20]. The proton is there decomposed into a pair of a quark and a diquark. The average radius

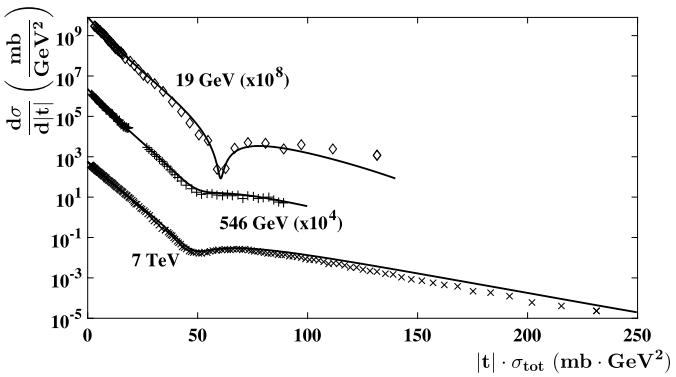

Fig. 3. The differential elastic cross sections from our model for c.m.s energies of 19 GeV, 546 GeV and 7 TeV shown as a function of the ($|t| \times \sigma_{\mathrm{tot}}$) according to the suggestion of Eq. (11) compared with the measurements [4,9,12,19,33].

of the diquark distribution is significantly larger than that of the remaining single quark constituent. This simple idea is improved by the addition of the real part to the forward scattering amplitude and is examined by Csorgo and Nemes in Ref. [38] where it is shown that it can be successfully applied to the LHC energies of 7 TeV.

The other model of Islam, Luddy and Prokudin [49] describes the high energy proton–proton scattering assuming that nucleons have the hard inner core and the diffractive, soft outer cloud. The amplitude is the sum of the hard core–core scattering dominated at high $|t|$ values and the soft, low $|t|$ scattering of the overlapping clouds.

4. Results

Proton profiles shown in Fig. 2 were obtained with the adjustment procedure using the data of the differential elastic cross sections. We pay our attention to reproduce the main characteristics of the measured distributions:

- the slope at the low momentum transfer,
- the position of the first diffractive peak,
- the behavior after the peak and the slope at high momentum transfers.

The accuracy of the obtained data description for the three characteristic energies is shown in Fig. 3. We have presented our model predictions of the differential cross section distribution as a function of the product of the value of the momentum transfer and the total cross section which follows the idea of Ref. [34] given by Eq. (11).

Four parameters $m_{1,2}$ and $c_{1,2}$ were found for ten energy data sets starting from $\sqrt{s} = 20$ GeV, through five energies of ISR (23–62 GeV) an SPS point at 546 GeV, two Tevatron measurements at 0.6 and 2 TeV and the LHC data set measured at c.m.s. energy of 7 TeV. All the parameter values adjusted individually for each energy are given in Figs. 4 (a) and (b) as solid symbols. Recent LHC data obtained at the energy of 8 TeV are not included for the fitting procedure of our model because of the low momentum transfer range ($0.029 < |t| < 0.195$) [13] covered. Anyway, we tried to use them for the slope of the differential elastic cross section determination and the result is given in Fig. 5.

Comparing the values obtained for different energies we see a clear regularity. The results in Fig. 4 suggest a simple form of the low and high energy asymptotics for all the four parameters. It seems that the dependence tends to get linear in logarithmic scale for all four parameter cases. The lines are shown in Fig. 4 by the

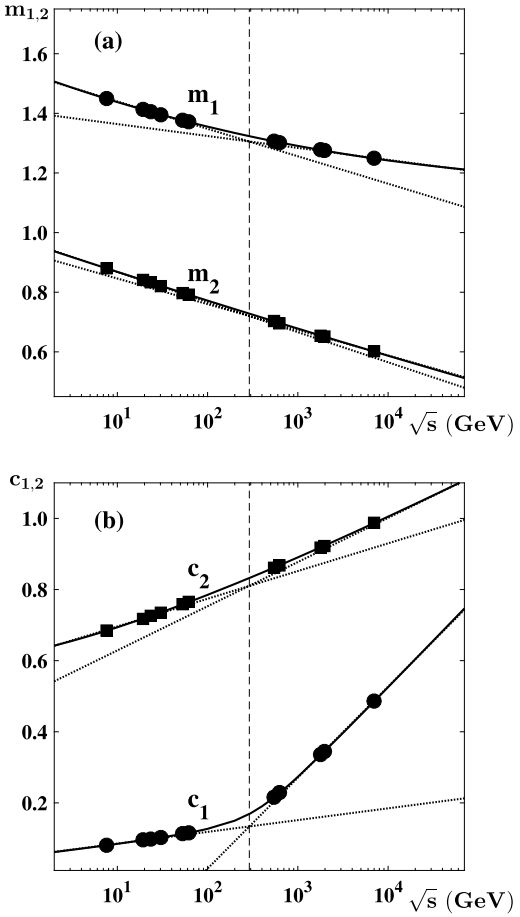

Fig. 4. The values of adjusted parameters $m_{1,2}$ (a) and $c_{1,2}$ (b) are shown by the solid symbols. Dashed lines show asymptotic linear energy dependencies (for high and low energies) of all parameters. Solid lines are the smooth overall energy dependencies eventually adopted for the results presented in this work (Figs. 2, 3, 5 and 6).

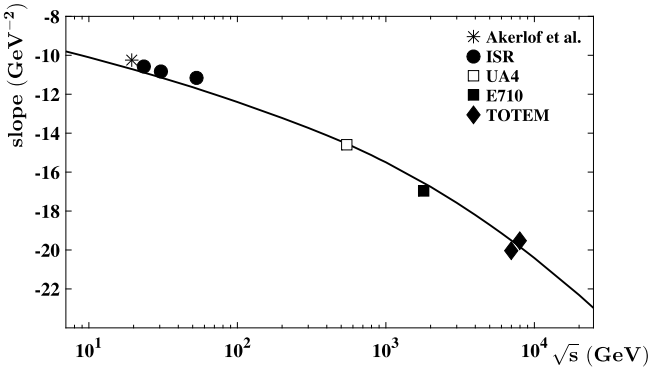

Fig. 5. Calculated slopes of the elastic differential cross sections as a function of interaction energy. Line shows our model predictions, points are fits to the experimental results from [3,4,7,10,13,19,33] in the range of $0.1 < |t| < 0.3$ GeV^2.

dotted lines. The relatively small number of high energy elastic scattering experiments providing differential elastic cross section distributions of the quality and range good enough for our model parameter estimation procedure does not allow us to make strong conclusions, but the obtained evidence looks quite impressive. Additionally the genuine character of the proposed parameterization is confirmed by the fact that the change from low to high energy regime is located at approximately the same energy point. The chance coincidence of such behavior is rather unbearable.

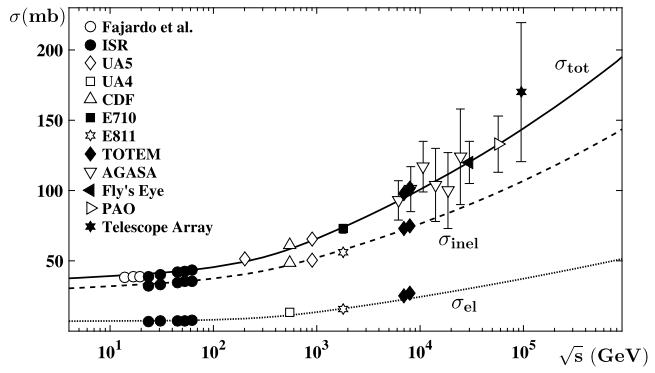

Fig. 6. Values of the elastic, inelastic and total cross section calculated with our model as a function of the interaction energy compared with the measurements. Solid line represents total cross section, dashed inelastic and dotted line elastic cross section predictions. Points are experimental results from Refs. [1–3,5,6,8,10,11,15,18,32,43,53].

The asymptotic dependencies and the smooth connections between them shown in all four cases in Fig. 4 by the solid curves were used to obtain our model predictions presented in Figs. 2, 3, 5 and 6.

Using the values of the parameters given by the solid lines in Fig. 4 some detailed characteristics of the proton–proton scattering can be obtained. One of them is the low $|t|$ slope. It can be easily obtained from published data and we present them with our model prediction in Fig. 5.

The most important characteristics of the proton–proton scattering are the integrated cross sections (total, elastic and inelastic). With our model and the parameters as described in Fig. 4 they can be calculated.

Results are given in Fig. 6. Our model predictions are compared there with the data from accelerator measurements and with the results obtained by the cosmic ray experiments: Fly's Eye [18], PAO [3] and Telescope Array [1]. As it can be seen, the extrapolated model predictions are in agreement with high-energy cosmic ray data.

The numerical model predictions for the energies higher than measured so far ones starting from the LHC 14 TeV up to UHECR energies, are given in the Table 1. They are compared with some values existing in the literature.

5. Summary

We have developed a modified simple optical model of proton–proton scattering with four model parameters, which allows us to describe the hadronic matter distribution of colliding protons. Values of all the parameters were adjusted to the elastic scattering data in the wide range of energies from stationary target experiment below ISR to the 7 TeV energy of LHC $|t|$ distribution data. Using the eikonal parameterization the correct description of the total and elastic cross sections, the elastic slope and the differential elastic cross section at large values of momentum transfer have been found.

However, the satisfactory description of the existing scattering data was not the main result of our work. We have found additionally a smooth and very simple behavior of all parameter's energy dependence.

In particular, we found that for the low and the high energies there are asymptotic regimes which seem to be linear in the logarithmic scale of the available interaction energy $\sqrt{s}$. Moreover, the change of the low energy to the high energy regime is found to be located for all the model parameters at around the same point on the energy scale – $\sqrt{s} = 300$ GeV. Its more accurate estimation is impossible because of the lack of the data in this particular energy range.

These facts constitute the solid base for the extrapolation of the scattering cross sections above energies available from accelerator measurements at present, up to the ultra-high energies observed in cosmic rays.

In agreement with "BEL" behavior our model shows that the proton becomes blacker and larger as the energy increases. Increasing of c_1 parameter which represents normalization of inner core of the proton shows that blackening is faster above $\sqrt{s} = 300$ GeV. Other three parameters indicate also a slow increase of hadronic radius. Thanks to the new parameterization of the hadronic matter distribution we obtain better agreement with scattering differential cross section accelerator data for higher momenta transfers for all available energies.

Using our model, we calculate the predictions for the pp total cross section at $\sqrt{s} = 14$ TeV, and 57 TeV, and they are $\sigma_{pp}^{tot} = 105.56$ mb and 132.66 mb, respectively. For the inelastic cross sections the respective values are: $\sigma_{pp}^{inel} = 79.71$ mb and 98.69 mb.

Appendix A. Supplementary material

Supplementary material related to this article can be found online at http://dx.doi.org/10.1016/j.physletb.2016.08.064.

References

[1] R.U. Abbasi, et al., Telescope Array Collaboration, Measurement of the proton-air cross section with Telescope Array's Middle Drum detector and surface array in hybrid mode, Phys. Rev. D 92 (2015) 032007, http://dx.doi.org/10.1103/PhysRevD.92.032007, arXiv:1505.01860.

[2] F. Abe, et al., CDF Collaboration, Measurement of the antiproton–proton total cross section at $\sqrt{s} = 546$ and 1800 GeV, Phys. Rev. D 50 (1994) 5550–5561, http://dx.doi.org/10.1103/PhysRevD.50.5550.

[3] P. Abreu, et al., The Pierre Auger Collaboration, Measurement of the proton-air cross section at $\sqrt{s} = 57$ TeV with the Pierre Auger Observatory, Phys. Rev. Lett. 109 (2012) 062002, http://dx.doi.org/10.1103/PhysRevLett.109.062002.

[4] C.W. Akerlof, et al., Hadron–proton elastic scattering at 50-GeV/c, 100-GeV/c and 200-GeV/c momentum, Phys. Rev. D 14 (1976) 2864, http://dx.doi.org/10.1103/PhysRevD.14.2864.

[5] G.J. Alner, et al., UA5 Collaboration, Antiproton–proton cross sections at 200 and 900 GeV c.m. energy, Z. Phys. C 32 (1986) 153–161, http://dx.doi.org/10.1007/BF01552491.

[6] U. Amaldi, K. Schubert, Impact parameter interpretation of proton–proton scattering from a critical review of all ISR data, Nucl. Phys. B 166 (1980) 301–320.

[7] N.A. Amos, et al., E-710 Collaboration, $\bar{p}p$ elastic scattering at $\sqrt{s} = 1.8$ TeV from $|t| = 0.034$-GeV/c^2 to 0.65-GeV/c^2, Phys. Lett. B 247 (1990) 127–130, http://dx.doi.org/10.1016/0370-2693(90)91060-O.

[8] N.A. Amos, et al., E710 Collaboration, Measurement of ρ, the ratio of the real to imaginary part of the $\bar{p}p$ forward elastic scattering amplitude, at $\sqrt{s} = 1.8$-TeV, Phys. Rev. Lett. 68 (1992) 2433–2436, http://dx.doi.org/10.1103/PhysRevLett.68.2433.

[9] G. Antchev, et al., TOTEM Collaboration, Proton–proton elastic scattering at the LHC energy of $\sqrt{s} = 7$ TeV, Europhys. Lett. 95 (2011) 41001.

[10] G. Antchev, et al., TOTEM Collaboration, Luminosity-independent measurement of the proton–proton total cross section at $\sqrt{s} = 8$ TeV, Phys. Rev. Lett. 111 (2013) 012001, http://dx.doi.org/10.1103/PhysRevLett.111.012001.

[11] G. Antchev, et al., TOTEM Collaboration, Luminosity-independent measurements of total, elastic and inelastic cross-sections at $\sqrt{s} = 7$ TeV, Europhys. Lett. 101 (2013) 21004, http://dx.doi.org/10.1209/0295-5075/101/21004.

[12] G. Antchev, et al., TOTEM Collaboration, Measurement of proton–proton elastic scattering and total cross-section at $\sqrt{s} = 7$ TeV, Europhys. Lett. 101 (2013) 21002.

[13] G. Antchev, et al., TOTEM Collaboration, Evidence for non-exponential elastic proton–proton differential cross-section at low $|t|$ and $\sqrt{s} = 8$ TeV by TOTEM, Nucl. Phys. B 899 (2015) 527–546, http://dx.doi.org/10.1016/j.nuclphysb.2015.08.010, arXiv:1503.08111.

[14] C. Augier, et al., UA4/2 Collaboration, A precise measurement of the real part of the elastic scattering amplitude at the S$\bar{p}$pS, Phys. Lett. B 316 (1993) 448–454.

[15] C. Avila, et al., E811 Collaboration, A measurement of the proton–antiproton total cross-section at $\sqrt{s} = 1.8$-TeV, Phys. Lett. B 445 (1999) 419–422, http://dx.doi.org/10.1016/S0370-2693(98)01421-X.

[16] R. Ávila, S. Campos, M. Menon, J. Montanha, Phenomenological analysis connecting proton–proton and antiproton–proton elastic scattering, Eur. Phys. J. C 47 (2006) 171–186, http://dx.doi.org/10.1140/epjc/s2006-02530-x.

[17] R. Ávila, M. Menon, Eikonal zeros in the momentum transfer space from proton–proton scattering: an empirical analysis, Eur. Phys. J. C 54 (2008) 555–576, http://dx.doi.org/10.1140/epjc/s10052-008-0542-5.

[18] R.M. Baltrusaitis, G.L. Cassiday, J.W. Elbert, P.R. Gerhardy, S. Ko, E.C. Loh, Y. Mizumoto, P. Sokolsky, D. Steck, Total proton–proton cross section at $s^{\frac{1}{2}} = 30$ TeV, Phys. Rev. Lett. 52 (1984) 1380–1383, http://dx.doi.org/10.1103/PhysRevLett.52.1380.

[19] R. Battiston, et al., UA4 Collaboration, Proton–anti-proton elastic scattering at four momentum transfer up to 0.5-GeV^2 at the CERN SPS collider, Phys. Lett. B 127 (1983) 472, http://dx.doi.org/10.1016/0370-2693(83)90296-4, 141 (1983).

[20] A. Bialas, A. Bzdak, Constituent quark and diquark properties from small angle proton–proton elastic scattering at high energies, Acta Phys. Pol. B 38 (2007) 159–168, arXiv:hep-ph/0612038.

[21] M. Block, Hadronic forward scattering: predictions for the large hadron collider and cosmic rays, Phys. Rep. 436 (2006) 71–215.

[22] M.M. Block, Ultrahigh energy predictions of proton-air cross sections from accelerator data: an update, Phys. Rev. D 84 (2011) 091501, http://link.aps.org/doi/10.1103/PhysRevD.84.091501.

[23] M.M. Block, R.N. Cahn, High-energy $p\bar{p}$ and pp forward elastic scattering and total cross sections, Rev. Mod. Phys. 57 (1985) 563–598, http://dx.doi.org/10.1103/RevModPhys.57.563.

[24] M.M. Block, L. Durand, P. Ha, F. Halzen, Eikonal fit to pp and $\bar{p}p$ scattering and the edge in the scattering amplitude, Phys. Rev. D 92 (2015) 014030, http://dx.doi.org/10.1103/PhysRevD.92.014030.

[25] M.M. Block, E.M. Gregores, F. Halzen, G. Pancheri, Photon–proton and photon–photon scattering from nucleon–nucleon forward amplitudes, Phys. Rev. D 60 (1999) 054024, http://dx.doi.org/10.1103/PhysRevD.60.054024.

[26] M.M. Block, F. Halzen, Forward hadronic scattering at 7 TeV: predictions for the LHC: an update, Phys. Rev. D 83 (2011) 077901, http://dx.doi.org/10.1103/PhysRevD.83.077901, arXiv:1102.3163.

[27] C. Bourrely, J.M. Myers, J. Soffer, T.T. Wu, High-energy asymptotic behavior of the Bourrely–Soffer–Wu model for elastic scattering, Phys. Rev. D 85 (2012) 096009, http://dx.doi.org/10.1103/PhysRevD.85.096009.

[28] C. Bourrely, J. Soffer, T.T. Wu, New impact picture for low- and high-energy proton–proton elastic scattering, Phys. Rev. D 19 (1979) 3249–3260, http://dx.doi.org/10.1103/PhysRevD.19.3249.

[29] C. Bourrely, J. Soffer, T.T. Wu, Impact-picture expectations for very high-energy elastic pp and $\bar{p}p$ scattering, Nucl. Phys. B 247 (1984) 15–28.

[30] C. Bourrely, J. Soffer, T.T. Wu, pp and $p\bar{p}$ elastic scattering at $\sqrt{s} = 0.55$ to 40 TeV, Phys. Rev. Lett. 54 (1985) 757–759, http://link.aps.org/doi/10.1103/PhysRevLett.54.757.

[31] C. Bourrely, J. Soffer, T.T. Wu, Determination of the forward slope in pp and $\bar{p}p$ elastic scattering up to LHC energy, Eur. Phys. J. C 71 (2011) 1601, http://dx.doi.org/10.1140/epjc/s10052-011-1601-x.

[32] M. Bozzo, et al., UA4 Collaboration, Measurement of the proton–anti-proton total and elastic cross-sections at the CERN SPS collider, Phys. Lett. B 147 (1984) 392–398, http://dx.doi.org/10.1016/0370-2693(84)90139-4.

[33] M. Bozzo, et al., UA4 Collaboration, Elastic scattering at the CERN SPS collider up to a four momentum transfer of 1.55-GeV^2, Phys. Lett. B 155 (1985) 197–202, http://dx.doi.org/10.1016/0370-2693(85)90985-2.

[34] P. Brogueira, J.D. de Deus, Evolution equation for soft physics at high energy, J. Phys. G, Nucl. Part. Phys. 37 (2010) 075006.

[35] P. Carvalho, A. Martini, M. Menon, Eikonal representation in the momentum-transfer space, Eur. Phys. J. C 39 (2005) 359–376, http://dx.doi.org/10.1140/epjc/s2004-02096-7.

[36] H. Cheng, T.T. Wu, Theory of high-energy diffraction scattering. I, Phys. Rev. D 1 (1970) 1069–1082, http://dx.doi.org/10.1103/PhysRevD.1.1069.

[37] T.T. Chou, C.N. Yang, Model of elastic high-energy scattering, Phys. Rev. 170 (1968) 1591–1596, http://dx.doi.org/10.1103/PhysRev.170.1591.

[38] T. Csörgő, F. Nemes, Elastic scattering of protons from $\sqrt{s} = 23.5$ GeV to 7 TeV from a generalized Bialas–Bzdak model, Int. J. Mod. Phys. A 29 (2014) 1450019, http://dx.doi.org/10.1142/S0217751X14500195, arXiv:1306.4217.

[39] I.M. Dremin, Elastic scattering of hadrons, Phys. Usp. 56 (2013) 3.

[40] D. Fagundes, M. Menon, G. Silva, Model-independent data reductions of elastic proton–proton scattering, Eur. Phys. J. C 71 (2011), http://dx.doi.org/10.1140/epjc/s10052-011-1637-y.

[41] D.A. Fagundes, M.J. Menon, P.V.R.G. Silva, On the rise of proton–proton cross-sections at high energies, J. Phys. G, Nucl. Part. Phys. 40 (2013) 065005, http://stacks.iop.org/0954-3899/40/i=6/a=065005.

[42] D.A. Fagundes, G. Pancheri, A. Grau, S. Pacetti, Y.N. Srivastava, Elastic pp scattering from the optical point to past the dip: an empirical parametrization from ISR to the LHC, Phys. Rev. D 88 (2013) 094019, http://dx.doi.org/10.1103/PhysRevD.88.094019.

[43] L.A. Fajardo, R. Majka, J.N. Marx, P. Némethy, L. Rosselet, J. Sandweiss, A. Schiz, A.J. Slaughter, C. Ankenbrandt, M. Atac, R. Brown, S. Ecklund, P.J. Gollon, J. Lach, J. MacLachlan, A. Roberts, G. Shen, Real part of the forward elastic nuclear amplitude for pp, $\bar{p}p$, π^+p, π^-p, K^+p, and K^-p scattering between 70 and 200 GeV/c, Phys. Rev. D 24 (1981) 46–65, http://dx.doi.org/10.1103/PhysRevD.24.46.

[44] A.A. Godizov, Current stage of understanding and description of hadronic elastic diffraction, AIP Conf. Proc. 1523 (2013).

[45] A. Grau, S. Pacetti, G. Pancheri, Y.N. Srivastava, Checks of asymptotia in pp elastic scattering at LHC, Phys. Lett. B 714 (2012) 70–75.

[46] R. Henzi, P. Valin, Towards a blacker, edgier and larger proton, Phys. Lett. B 132 (1983) 443–448, http://dx.doi.org/10.1016/0370-2693(83)90344-1.

[47] M.M. Islam, V. Innocente, T. Fearnley, G. Sanguinetti, High-energy $\bar{p}p$ and pp elastic scattering and nucleon structure, Europhys. Lett. 4 (1987) 189.

[48] M.M. Islam, R.J. Luddy, A.V. Prokudin, pp elastic scattering at LHC and nucleon structure, Mod. Phys. Lett. A 18 (2003) 743–752, http://dx.doi.org/10.1142/S0217732303009897.

[49] M.M. Islam, R.J. Luddy, A.V. Prokudin, Near forward pp elastic scattering at LHC and nucleon structure, Int. J. Mod. Phys. A 21 (2006) 1–41, http://dx.doi.org/10.1142/S0217751X06028473.

[50] L.L. Jenkovszky, A.I. Lengyel, D.I. Lontkovskyi, The pomeron and odderon in elastic, inelastic and total cross sections at the LHC, Int. J. Mod. Phys. A 26 (2011) 4755–4771, http://dx.doi.org/10.1142/S0217751X11054760, arXiv:1105.1202.

[51] V.A. Khoze, A.D. Martin, M.G. Ryskin, Elastic scattering and diffractive dissociation in the light of LHC data, Int. J. Mod. Phys. A 30 (2015) 1542004, http://dx.doi.org/10.1142/S0217751X1542004X.

[52] A.F. Martini, M.J. Menon, Multiple diffraction model for proton–proton elastic scattering and total cross section extrapolations to cosmic-ray energies, Phys. Rev. D 56 (1997) 4338–4349, http://dx.doi.org/10.1103/PhysRevD.56.4338.

[53] K. Olive, et al., Particle Data Group, Review of particle physics, Chin. Phys. C 38 (2014) 090001, http://dx.doi.org/10.1088/1674-1137/38/9/090001.

[54] J. Orear, R. Rubinstein, D.B. Scarl, D.H. White, A.D. Krisch, W.R. Frisken, A.L. Read, H. Ruderman, Large-angle pion–proton elastic scattering at high energies, Phys. Rev. 152 (1966) 1162–1170, http://dx.doi.org/10.1103/PhysRev.152.1162.

[55] V.A. Petrov, A.V. Prokudin, The first three pomerons..., Eur. Phys. J. C 23 (2002) 135–143, http://dx.doi.org/10.1007/s100520100838.

[56] R.J.N. Phillips, V.D. Barger, Model independent analysis of the structure in pp scattering, Phys. Lett. B 46 (1973) 412–414, http://dx.doi.org/10.1016/0370-2693(73)90154-8.

[57] M. Rybczyński, Z. Włodarczyk, The nucleon–nucleon collision profile and cross section fluctuations, J. Phys. G, Nucl. Part. Phys. 41 (2014) 015106.

[58] T. Wibig, Elastic scattering at 7 TeV and high-energy cross section for cosmic ray studies, J. Phys. G, Nucl. Part. Phys. 39 (2012) 085003.